

Harmonic generation and multiphoton ionization near an autoionizing resonance

G. Alber and P. Zoller

Institute for Theoretical Physics, University of Innsbruck, A-6020 Innsbruck, Austria

(Received 29 June 1982)

We theoretically study intensity-saturation effects in resonant harmonic generation and multiphoton ionization. A first laser excites a two-photon resonance which is coupled by a second laser to an autoionizing state. Starting from an effective Hamiltonian for the three resonant atomic states, we derive a set of equations for the density matrix of the gaseous medium and the electromagnetic field within a semiclassical framework. We present and discuss analytical and numerical solutions of these equations which show a variety of line profiles depending critically on the intensities of the incident laser pulses.

I. INTRODUCTION

An autoionizing state is an approximate bound state of a multielectron atom whose energy lies above the first ionization threshold. Due to configuration interaction, this state is unstable against ionization with one electron being ejected.¹⁻³

With the development of tunable dye lasers it has become possible to study the autoionizing resonances by multiphoton excitation.⁴⁻¹³ From the spectroscopic point of view this allowed to observe and classify with extreme accuracy autoionizing states which cannot be reached by one-photon vacuum ultraviolet (vuv) absorption spectroscopy from the atomic ground state.¹⁴ On the other hand, the high intensities and narrow spectral widths of laser radiation introduce the additional aspect to study the behavior of autoionizing states in strong laser fields.^{11,15} A bound-bound transition strongly driven by a near-resonant laser becomes saturated and undergoes ac-Stark splitting.¹⁶ The saturation behavior of an autoionizing transition in an intense laser, on the other hand, is complicated by the simultaneous presence of both the radiation field and the configuration interaction.¹⁷ Owing to the large decay widths of autoionizing states, relatively large laser powers (typically $\gtrsim 10^{10}$ W/cm²) are required to saturate a (one-photon) autoionizing transition. In the context of (multiphoton) ionization the weak-field Fano theory of autoionizing line shapes has recently been generalized to include intensity effects, manifesting themselves in a considerable distortion of the familiar Fano profiles of photoabsorption as a function of the intensity and interaction time.¹⁸⁻²⁰ There is some indication that recent multiphoton ionization experiments in alkaline-earth atoms have observed such effects.¹¹

While so far most of the theoretical work has concentrated on the ionization problem, these intensity effects are also observable in related processes. One example of particular relevance is harmonic generation which provides a source for coherent vuv light.²¹⁻²⁶ A typical scheme of a wave-mixing process of this type in an alkaline-earth atom is the following⁶: A first laser is tuned to a two-photon resonance; this avoids strong absorption at the fundamental frequency. A second laser then excites the electrons to states above the first ionization threshold. Scanning with this laser over the autoionizing resonances, one observes a considerable enhancement of harmonic production with lineshapes differing from those of photoionization. Most of these theoretical studies so far have only been concerned with weak-field excitations of the two-photon resonance and the autoionizing state, where an intensity-independent nonlinear susceptibility can be defined, neglecting saturation and induced ionization of the resonances as well as pulse propagation effects.^{7,8}

Motivated by present-day experimental possibilities, the purpose of this paper is to generalize the theory of nonlinear sum-frequency generation via a two-photon and autoionizing resonance including intensity-saturation effects. We thereby extend the pioneering work of Armstrong and Wynne,⁷ Armstrong and Beers,⁸ and Heller and Popov.²⁷ In view of the intimate relationship between harmonic generation above the ionization threshold and ionization, such a study must be complemented by an investigation of the competing process of two-photon resonant three-photon ionization near the autoionizing state.²⁸

This paper is organized as follows. In Sec. II we derive the density-matrix equations of our gaseous

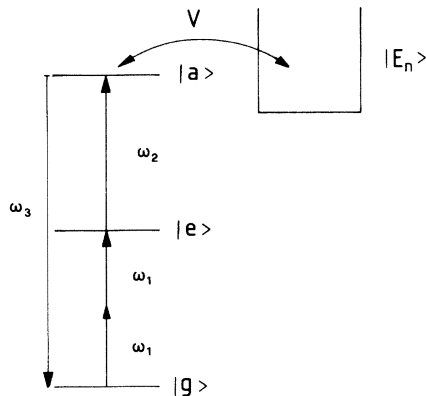


FIG. 1. Atomic configuration.

medium and the nonlinear atomic polarizations, which provide the source terms in the classical Maxwell equations for the two injected laser signals and the generated harmonic light. Pulse propagation effects are only included in terms of a phase-matching function, neglecting depletion of the fundamental light waves. Approximate analytical expressions for the energy of the harmonic radiation and ionization signal are derived in Secs. III and IV. These results are discussed and illustrated by numerical examples for various parameter combinations in Sec. V.

II. BASIC EQUATIONS

In this section we derive the basic density-matrix and Maxwell equations describing the process of (two-photon resonant) harmonic generation and multiphoton ionization near an autoionizing resonance. Figure 1 illustrates the atomic configuration which is studied in this paper. We consider a gas of atoms interacting with two laser beams with frequencies ω_1 and ω_2 . The first laser excites electrons from the ground state $|g\rangle$ to the two-photon resonance $|e\rangle$. The second laser is tuned to the one-photon transition from the excited state $|e\rangle$ to an autoionizing resonance $|a\rangle$ (where $|a\rangle$ denotes the bound-state part of the autoionizing state) which decays into a series of continua $|E_\alpha\rangle$ by configuration interaction. In addition, both $|e\rangle$ and $|a\rangle$ can be ionized by one photon of the first or second laser. From the autoionizing state the atoms can decay to their ground states, emitting vuv photons with frequency $\omega_3 = 2\omega_1 + \omega_2$. This process of harmonic generation competes with resonant three-photon ionization.

A typical experimental situation we have in mind is the following⁶: Alkaline-earth atoms with a $J=0$

ground state are excited to an autoionizing resonance. In harmonic generation, only autoionizing states with $J=1$ can be seen in the dipole approximation; these are the states known from (one-photon) absorption spectroscopy from the ground state. In multiphoton ionization, generally also higher-angular-momentum states become visible. To suppress the third harmonics at $3\omega_1$ and $3\omega_2$, both lasers are usually taken to be circularly polarized in opposite directions.

A. Density-matrix equations for the medium

The Hamiltonian $H = H_0 + V + D$ governing the time evolution of an atom in the gaseous medium consists of three parts. The configuration interaction is described by V , while $D = -\vec{\mu} \cdot \vec{E}(z, t)$ is the dipole interaction with the electromagnetic field, where

$$\vec{E}(z, t) = \sum_{j=1}^3 \vec{e}_j \mathcal{E}_j(z, t) \exp\{-i[\omega_j t - k_j(z, t)z]\} + \text{c.c.} \quad (2.1)$$

describes the three relevant modes of the electromagnetic field propagating in z direction. $\mathcal{E}_j(z, t)$ and $k_j(z, t)$ denote the slowly varying amplitudes and wave vectors at the position of the atom at the fundamental frequencies ω_1, ω_2 and the frequency of the generated harmonic $\omega_3 = 2\omega_1 + \omega_2$. The time evolution of the atom is determined from the above Hamiltonian using the following approximations (for mathematical details see Appendix):

(i) Following Fano's treatment of autoionization¹ we assume $|a\rangle$ to be an isolated autoionizing resonance interacting with the continua $|E_\alpha\rangle$ and all other bound states via the configuration interaction V . The bound states $|g\rangle$ and $|e\rangle$ are assumed to be exact eigenstates of the atomic Hamiltonian $H_0 + V$ [compare Appendix, Eq. (A5)].

(ii) The interaction of the radiation field with the atom is modeled by a three-level system with the states $|g\rangle, |e\rangle, |a\rangle$ in the rotating-wave approximation. The decay of the levels $|e\rangle$ and $|a\rangle$ into the continua by laser-induced ionization and configuration interaction is described by decay widths, which assumes that both the dipole and the configuration-interaction matrix elements from the bound states $|e\rangle$ and $|a\rangle$ to the continua $|E_\alpha\rangle$ are smoothly varying functions of the energy over the relevant energy range. Laser-induced transitions between the continua are neglected.¹⁷ These processes mainly redistribute the electron energies in the continua and are not expected to have any

significant effect on the line shapes of the atomic resonances which are of primary interest in this paper. Nonresonant atomic states coupled to $|g\rangle$, $|e\rangle$, or $|a\rangle$ by dipole matrix element give rise to quadratic Stark shifts of the states of our three-level

system. The interaction of the atom with the generated harmonic can to a good approximation be neglected for typical conversion efficiencies.

These approximations which define our model yield the following effective atomic Hamiltonian:

$$\begin{aligned}
 H_{\text{eff}} = & (\omega_g + \delta\omega_g) |g\rangle\langle g| + (\omega_e + \delta\omega_e - i\frac{1}{2}\gamma_e) |e\rangle\langle e| + [\omega_a + \delta\omega_a - i\frac{1}{2}(\gamma_a + \Gamma_a)] |a\rangle\langle a| \\
 & + \mu_{eg} \mathcal{E}_1^2 \exp\{-2i[\omega_1 t - k_1(z,t)z]\} |e\rangle\langle g| + \mu_{ge} \mathcal{E}_1^{*2} \exp\{2i[\omega_1 t - k_1(z,t)z]\} |g\rangle\langle e| \\
 & - \mu_{ae} \left[1 - \frac{i}{q_{ae}}\right] \mathcal{E}_2 \exp\{-i[\omega_2 t - k_2(z,t)z]\} |a\rangle\langle e| - \mu_{ea} \left[1 - \frac{i}{q_{ae}}\right] \mathcal{E}_2^* \exp\{i[\omega_2 t - k_2(z,t)z]\} |e\rangle\langle a|.
 \end{aligned} \tag{2.2}$$

Here ω_g, ω_e , and ω_a denote the energies of the levels $|g\rangle$, $|e\rangle$, and $|a\rangle$. The energy shift $\delta\omega$ of $|a\rangle$ due to the configuration interaction with all other atomic states has been included in the definition of ω_a . $\delta\omega_j$ with $j=g, e, a$ is the quadratic Stark shift of the level $|j\rangle$ induced by the first and second laser. γ_j with $j=e, a$ are the field-induced one-photon ionization widths of $|e\rangle$ and $|a\rangle$. In terms of the dynamic (complex) polarizabilities defined by

$$\alpha_k(\omega_1) = \alpha'_k(\omega_1) + i\alpha''_k(\omega_1) = - \left\langle k \left| \left[\frac{\vec{\mu} \cdot \vec{e}_1}{\omega_k - \omega_1 - H_A + i\epsilon} \frac{1}{\vec{\mu} \cdot \vec{e}_1^* + \vec{\mu} \cdot \vec{e}_1^*} \frac{1}{\omega_k + \omega_1 - H_A + i\epsilon} \vec{\mu} \cdot \vec{e}_1 \right] \right| k \right\rangle \tag{2.3}$$

for an atomic state $|k\rangle$, the Stark shift of the ground state may be written as $\delta\omega_g = -\alpha'_g(\omega_1) |\mathcal{E}_1|^2 - \alpha'_g(\omega_2) |\mathcal{E}_2|^2$. The shift and width of the two-photon resonance $|e\rangle$ is given by

$$\delta\omega_e - i\frac{1}{2}\gamma_e = -\alpha_e(\omega_1) |\mathcal{E}_1|^2 - \bar{\alpha}_e(\omega_2) |\mathcal{E}_2|^2.$$

The bar on $\bar{\alpha}_e(\omega_2)$ indicates that in the infinite summation over the atomic states represented by the resolvents in Eq. (2.3) the (divergent) contribution in the second term from the autoionizing state $|a\rangle$ should be projected out according to

$$\bar{\alpha}_e(\omega_2) = - \left\langle e \left| \left[\frac{\vec{\mu} \cdot \vec{e}_2}{\omega_e - \omega_2 - H_A} \frac{1}{\vec{\mu} \cdot \vec{e}_2^* + \vec{\mu} \cdot \vec{e}_2^*} Q_a \frac{1}{\omega_e + \omega_2 - H_A + i\epsilon} Q_a \vec{\mu} \cdot \vec{e}_2 \right] \right| e \right\rangle, \tag{2.4}$$

with $Q_a = 1 - |a\rangle\langle a|$; this coupling is treated explicitly in our effective Hamiltonian equation (2.2). In a similar way we find for the shift and width of the autoionizing state,

$$\begin{aligned}
 \delta\omega_a - i\frac{1}{2}\gamma_a = & \left\langle \psi_a^- \left| \left[\frac{\vec{\mu} \cdot \vec{e}_1^*}{\omega_a + \omega_1 - H_A + i\epsilon} \vec{\mu} \cdot \vec{e}_1 + \vec{\mu} \cdot \vec{e}_1 \frac{1}{\omega_a - \omega_1 - H_A + i\epsilon} \vec{\mu} \cdot \vec{e}_1^* \right] \right| \mathcal{E}_1 \right|^2 \\
 & + \left[\frac{\vec{\mu} \cdot \vec{e}_2^*}{\omega_a + \omega_2 - H_A + i\epsilon} \vec{\mu} \cdot \vec{e}_2 \right. \\
 & \left. + \vec{\mu} \cdot \vec{e}_2 Q_e \frac{1}{\omega_a - \omega_2 - H_A + i\epsilon} Q_e \vec{\mu} \cdot \vec{e}_2^* \right] |\mathcal{E}_2|^2 \left| \psi_a^+ \right\rangle,
 \end{aligned} \tag{2.5}$$

where $Q_e = 1 - |e\rangle\langle e|$ again points out that the contribution from $|e\rangle$ should be projected out in the first term of Eq. (2.3) in analogy to Eq. (2.4). The expressions for the dressed atomic states $|\psi_a^\pm\rangle$ are given in the Appendix [see Eq. (A6)]. Note the different signs of $|\psi_a^\pm\rangle$ in Eq. (2.5) and the polarizabilities in Eqs. (A6), (A7), and (2.19);

zabilities in Eqs. (A6), (A7), and (2.19);

$$\Gamma_a = 2\pi \sum_{\alpha} |\langle E_{\alpha} | V | a \rangle|^2_{E_{\alpha} = \omega_a} \tag{2.6}$$

is the autoionization width of level $|a\rangle$. The effective two-photon bound-bound matrix element of the

transition $|q\rangle \rightarrow |e\rangle$ is given by

$$\mu_{eq} = \left\langle e \left| \vec{\mu} \cdot \vec{e}_1 \frac{1}{\omega_g + \omega_1 - H_A} \vec{\mu} \cdot \vec{e}_1 \right| g \right\rangle. \quad (2.7)$$

The dipole matrix element for the resonant excitation step $|e\rangle \rightarrow |a\rangle$ is

$$\mu_{ae} = \langle \phi_a | \vec{\mu} \cdot \vec{e}_2 | e \rangle, \quad (2.8)$$

with

$$|\phi_a\rangle = |a\rangle + P \frac{1}{\omega_a - H_A} Q_a V |a\rangle.$$

The Fano parameter¹

$$q_{ae} = \frac{\mu_{ae}}{\pi \sum_{\alpha} V_{aE_{\alpha}} \mu_{E_{\alpha}e}} \bigg|_{E_{\alpha}=\omega_a}, \quad (2.9)$$

with

$$\mu_{E_{\alpha}e} = \langle E_{\alpha} | \vec{\mu} \cdot \vec{e}_2 | e \rangle \text{ and } V_{aE_{\alpha}} = \langle a | V | E_{\alpha} \rangle,$$

characterizes the interference in the autoionization step. Defining a correlation coefficient²

$$\rho_{ae} = \sum_{\alpha} V_{aE_{\alpha}} \mu_{E_{\alpha}e} \left[\sum_{\alpha} |V_{aE_{\alpha}}|^2 \right]^{-1/2} \left[\sum_{\alpha} |\mu_{E_{\alpha}e}|^2 \right]^{-1/2} \quad (2.10)$$

which is one ($|\rho_{ea}| = 1$), if only one continuum participates, and whose modulus is smaller than 1 for a decay into several continua, we obtain the relation

$$\gamma_e^{(2)} = |2\mu_{ae} \mathcal{E}_2|^2 / (\rho_{ae} q_{ae})^2 \Gamma_a \quad (2.11)$$

for the field-induced ionization rate of the excited state $|e\rangle$ due to the second laser.

From the effective Hamiltonian (2.2) we derive the density-matrix equations describing the properties of the gaseous medium

$$\begin{aligned} \left[\frac{d}{dt} + \gamma_a + \Gamma_a + \frac{1}{\tau_a} \right] \rho_{aa} &= 2 \operatorname{Im}[\mu_{ea} (1 + i/q_{ea}) \mathcal{E}_2^* \bar{\rho}_{ae}], \\ \left[\frac{d}{dt} + \gamma_e + \frac{1}{\tau_e} \right] \rho_{ee} - \frac{1}{\tau_{ae}} \rho_{aa} &= -2 \operatorname{Im}[\mu_{ge} \mathcal{E}_1^{*2} \bar{\rho}_{eg} + \mu_{ea} (1 - i/q_{ea}) \mathcal{E}_2^* \bar{\rho}_{ae}], \\ \left[\frac{d}{dt} - i\Delta_1 - i\Delta_2 + \frac{1}{2} \left[\gamma_a + \Gamma_a + \frac{1}{\tau_a} \right] + \frac{1}{T_{ag}} \right] \bar{\rho}_{ag} &= i\mu_{ae} (1 - i/q_{ae}) \mathcal{E}_2 \bar{\rho}_{eg} + i\mu_{eg} \mathcal{E}_1^2 \bar{\rho}_{ae}, \\ \left[\frac{d}{dt} - i\Delta_2 + \frac{1}{2} \left[\gamma_e + \gamma_a + \Gamma_a + \frac{1}{\tau_a} + \frac{1}{\tau_e} \right] + \frac{1}{T_{ae}} \right] \bar{\rho}_{ae} &= i\mu_{ae} (1 - i/q_{ae}) \mathcal{E}_2 \rho_{ee} - i\mu_{ae} (1 + i/q_{ae}) \mathcal{E}_2 \rho_{aa} \\ &+ i\mu_{ge} \mathcal{E}_1^{*2} \bar{\rho}_{ag}, \end{aligned} \quad (2.12)$$

$$\begin{aligned} \left[\frac{d}{dt} - i\Delta_1 + \frac{1}{2} \left[\gamma_e + \frac{1}{\tau_e} \right] + \frac{1}{T_{eg}} \right] \bar{\rho}_{eg} &= -i\mu_{eg} \mathcal{E}_1^2 (\rho_{gg} - \rho_{ee}) + i\mu_{ea} (1 - i/q_{ea}) \mathcal{E}_2^* \bar{\rho}_{ag}, \\ \frac{d}{dt} \rho_{gg} - \frac{1}{\tau_{ag}} \rho_{aa} - \frac{1}{\tau_e} \rho_{ee} &= 2 \operatorname{Im}(\mu_{ge} \mathcal{E}_1^{*2} \bar{\rho}_{eg}), \end{aligned}$$

where we have used the abbreviation $\rho_{ij} \equiv \rho_{ij}(z, t)$ and neglected the inhomogeneous broadening due to the atomic motion in the gas. The various τ 's describe the effects of spontaneous decay and atomic collisions and have been added phenomenologically. The bars on the off-diagonal elements indicate the transformation to slowly varying variables:

$$\Delta_1 = 2\omega_1 + (\omega_g + \delta\omega_g) - (\omega_e + \delta\omega_e)$$

and

$$\Delta_2 = \omega_2 + (\omega_e + \delta\omega_e) - (\omega_a + \delta\omega_a)$$

denote the dynamic detunings.

For the following it will be convenient to define

$$\beta_{ag} = \frac{\Gamma_a}{\gamma_a + \Gamma_a + \frac{1}{\tau_a} + \frac{2}{T_{ag}}}, \quad (2.13)$$

$$\beta_{ae} = \frac{\Gamma_a}{\gamma_e + \gamma_a + \Gamma_a + \frac{1}{\tau_e} + \frac{1}{\tau_a} + \frac{2}{T_{ae}}},$$

and

$$\beta_{eg} = \frac{\gamma_e^{(2)}}{\gamma_e + \frac{1}{\tau_e} + \frac{2}{T_{eg}}},$$

where in practice β_{ag} is expected to be close to 1. Note that if Γ_a becomes comparable to the spontaneous decay width of $|a\rangle$ autoionization and spontaneous decay are no longer additive processes,^{29,30} as is implicitly assumed in Eq. (2.12).

The total ionization probability of the atom after the interaction time T follows from the solution of Eq. (2.12):

$$P(T) = 1 - \rho_{gg}(T) - \rho_{ee}(T) - \rho_{aa}(T). \quad (2.14)$$

If the ionized electrons are measured after a time long compared to the lifetime of $|a\rangle$, Eq. (2.14) has to be replaced by¹⁹

$$P_3(z, t) = [\alpha_g(\omega_3)\rho_{gg}(z, t) + \alpha_e(\omega_3)\rho_{ee}(z, t) + \alpha_a(\omega_3)\rho_{aa}(z, t)]\mathcal{E}_3(z, t) + [\xi_{ge}\mathcal{E}_2(z, t)\bar{\rho}_{eg}(z, t) + \mu_{ga}(1 - i/q_{ga})\bar{\rho}_{ag}(z, t)]\exp[-i\Delta k(z, t)z]. \quad (2.17)$$

The coefficient multiplying \mathcal{E}_3 contributes to the complex index of refraction. The ground-state polarizability is

$$\alpha_g(\omega_3) = -\left\langle g \left| \left[\vec{\mu} \cdot \vec{e}_3 \frac{1}{\omega_g - \omega_3 - H_A} \vec{\mu} \cdot \vec{e}_3^* + \vec{\mu} \cdot \vec{e}_3^* Q_a \frac{1}{\omega_g + \omega_3 - H_A + i\epsilon} Q_a \vec{\mu} \cdot \vec{e}_3 \right] \right| g \right\rangle - \frac{\mu_{ag}^2 (1 - i/q_{ag})^2}{\Delta_1 + \Delta_2 + i\frac{1}{2}\Gamma_a/\beta_{ag}}. \quad (2.18)$$

The first two terms describe the contribution from the nonresonant states including the continua. The third term is due to the presence of the autoionizing state, giving rise to a Fano-type resonance profile. A similar expression is found for $\alpha_a(\omega_3)$,

$$\alpha_a(\omega_3) = -\left\langle \psi_a^+ \left| \left[\vec{\mu} \cdot \vec{e}_3 Q_g \frac{1}{\omega_a - \omega_3 - H_A} Q_g \vec{\mu} \cdot \vec{e}_3^* + \vec{\mu} \cdot \vec{e}_3^* \frac{1}{\omega_a + \omega_3 - H_A + i\epsilon} \vec{\mu} \cdot \vec{e}_3 \right] \right| \psi_a^+ \right\rangle - \frac{\mu_{ag}^2 |1 - i/q_{ag}|^2}{-(\Delta_1 + \Delta_2) + i\frac{1}{2}\Gamma_a/\beta_{ag}}, \quad (2.19)$$

$$P(T) = 1 - \rho_{gg}(T) - \rho_{ee}(T) - \frac{1/\tau_a}{1/\tau_a + \Gamma_a} \rho_{aa}(T). \quad (2.15)$$

B. Maxwell equations

The polarization of the medium, as calculated from the density-matrix equations, provides the source terms in the Maxwell equations for the electromagnetic field. Decomposing the electric field according to Eq. (2.1) the first-order Maxwell equations for the slowly varying complex electric field amplitudes read

$$\left[\frac{\partial}{\partial z} + \frac{1}{c} \frac{\partial}{\partial t} \right] \mathcal{E}_k(z, t) = i \frac{\omega_k N}{2\epsilon_0 c} P_k(z, t), \quad k = 1, 2, 3. \quad (2.16)$$

N is the atomic density, assumed to be independent of z . $P_k(z, t)$ are the slowly varying polarizations. The equations for $\mathcal{E}_1(z, t)$ and $\mathcal{E}_2(z, t)$ describe the propagation of the incident light waves in the medium. Propagation effects, such as depletion, are of no concern in the present paper; they are negligible for short cells, smaller than a characteristic absorption length defined below. The polarization $P_3(z, t)$, which is responsible for the generation of the harmonic, is given by (see Appendix)

while $\alpha_e(\omega_3)$ is given by Eq. (2.3). Here, $\mu_{ga} = \langle g | \vec{\mu} \cdot \vec{e}_3^* | \phi_a \rangle$ is the dipole matrix element for the transition $|g\rangle \rightarrow |a\rangle$, and q_{ga} and ρ_{ga} are the corresponding Fano parameter and correlation coefficient defined in analogy with Eqs. (2.9) and (2.10).

The nonlinear part of the polarization consists of two contributions. The first term corresponds to the excitation of the two-photon resonance, followed by the absorption of a photon of frequency ω_2 and the emission of a photon at the generated harmonic frequency ω_3 via the nonresonant states or the continua described by ξ_{ge} , where

$$\xi_{ge} = \xi(1 - i/q_{ge}) \quad (2.20)$$

with

$$\xi = - \left\langle g \left| \left[\vec{\mu} \cdot \vec{e}_2 \frac{1}{\omega_g - \omega_2 - H_A} \vec{\mu} \cdot \vec{e}_3^* + \vec{\mu} \cdot \vec{e}_3^* Q_a P \frac{1}{\omega_g + 2\omega_1 + \omega_2 - H_A} Q_a \vec{\mu} \cdot \vec{e}_2 \right] \right| e \right\rangle$$

and

$$q_{ge} = \frac{-\xi}{\pi \sum_{\alpha} \langle g | \vec{\mu} \cdot \vec{e}_3^* | E_{\alpha} \rangle \langle E_{\alpha} | \vec{\mu} \cdot \vec{e}_2 | e \rangle} \Bigg|_{E_{\alpha} = \omega_{\alpha}},$$

where P denotes the principal value of the integral involved. The second part involves the resonant contribution from the autoionizing state. For a Doppler-broadened medium, the polarization $P_3(z, t)$ in Eq. (2.16) has to be averaged over the velocity distribution of the atoms in the gas.

For short cells, depletion of the two incident laser beams may be neglected. This allows us to approximate $\mathcal{E}_j(z, t)$, $j=1,2$, with the retarded time $\tau = t - z/c$ by its boundary value $\mathcal{E}_j(z=0, \tau)$ in the density-matrix equations (2.12) and in the polarization $P_3(z, t)$. In this way we find for the energy of the generated harmonic

$$\begin{aligned} U_3 &= 2\epsilon_0 c \int_{-\infty}^{\infty} d\tau |\mathcal{E}_3(L, \tau)|^2 \\ &= \frac{\omega_3^2}{2\epsilon_0 c} (NL)^2 \int_{-\infty}^{\infty} d\tau |\xi_{ge} \bar{\rho}_{eg}(0, \tau) \mathcal{E}_2(0, \tau) \\ &\quad + \mu_{ga} (1 - i/q_{ga}) \bar{\rho}_{ag}(0, \tau)|^2 F(\Delta k(0, \tau)L, \sigma(0, \tau)L), \end{aligned} \quad (2.21)$$

where L is the length of the cell;

$$F(\Delta k(0, \tau)L, \sigma(0, \tau)L) = \frac{1}{4} \frac{1 + \exp[-2\sigma(z, \tau)L] - 2 \exp[-\sigma(z, \tau)L] \cos[\Delta k(z, \tau)L]}{\left[\frac{\sigma(z, \tau)L}{2} \right]^2 + \left[\frac{\Delta k(z, \tau)L}{2} \right]^2} \Bigg|_{z=0} \quad (2.22)$$

represents the characteristic phase-matching function with the phase mismatch

$$\Delta k(z, \tau) = k_3(z, \tau) - 2k_1(z, \tau) - k_2(z, \tau). \quad (2.23)$$

The wave vectors $k_j(z, \tau)$, $j=1,2,3$, are defined by

$$k_j(z, \tau) = \frac{\omega_j}{2\epsilon_0 c} N \operatorname{Re}[\alpha_g(\omega_j)\rho_{gg}(z, \tau) + \alpha_e(\omega_j)\rho_{ee}(z, \tau) + \alpha_a(\omega_j)\rho_{aa}(z, \tau)] + \frac{\omega_j}{c}; \quad (2.24)$$

$$\sigma(z, \tau) = \frac{\omega_3}{2\epsilon_0 c} N \operatorname{Im}[\alpha_g(\omega_3)\rho_{gg}(z, \tau) + \alpha_e(\omega_3)\rho_{ee}(z, \tau) + \alpha_a(\omega_3)\rho_{aa}(z, \tau)] \quad (2.25)$$

is the absorption coefficient of the generated harmonic. If a buffer gas is used to obtain phase matching appropriate terms on the right-hand side of Eqs. (2.23) and (2.24) have to be added describing the change of the index of refraction.

Equation (2.1) for the energy of the generated harmonic radiation together with Eq. (2.12) for the density matrix of the medium are the basic equations which are studied in this paper.

For completeness we also give the expressions for the polarizations $P_1(z,t)$ and $P_2(z,t)$ at the first and second laser frequency,

$$P_1(z,t) = [\alpha_g(\omega_1)\rho_{gg}(z,t) + \alpha_e(\omega_1)\rho_{ee}(z,t) + \alpha_a(\omega_1)\rho_{aa}(z,t)]\mathcal{E}_1(z,t) - 2\mu_{ge}\bar{\rho}_{eg}(z,t)\mathcal{E}_1^*(z,t) \quad (2.26)$$

and

$$P_2(z,t) = [\alpha_g(\omega_2)\rho_{gg}(z,t) + \bar{\alpha}_e(\omega_2)\rho_{ee}(z,t) + \bar{\alpha}_a(\omega_2)\rho_{aa}(z,t)]\mathcal{E}_2(z,t) + \mu_{ea}(1-i/q_{ea})\bar{\rho}_{ae}(z,t), \quad (2.27)$$

where the contributions involving the generated harmonic field amplitude have been neglected. The expressions for the atomic polarizabilities are given in Sec. II A and in the Appendix.

The inverse of the imaginary part of the right-hand side of the equations for \mathcal{E}_1 and \mathcal{E}_2 , evaluated at $z=0$, provides an estimate of the characteristic absorption lengths of the incident light waves.

III. WEAK COUPLING TO THE AUTOIONIZING STATE

If the laser-induced coupling between the two-photon resonance and the autoionizing state is weak, the adiabatic elimination of the density-matrix elements referring to the autoionizing states reduces Eq. (2.12) to Bloch-type equations for the two-level system $|g\rangle, |e\rangle$:

$$\begin{aligned} \left[\frac{d}{dt} + \gamma_e^F + \frac{1}{\tau_e} \right] \rho_{ee} &= -2 \operatorname{Im}(\mu_{ge} \mathcal{E}_1^{*2} \bar{\rho}_{eg}), \\ \frac{d}{dt} \rho_{gg} - \frac{1}{\tau_e} \rho_{ee} &= 2 \operatorname{Im}(\mu_{ge} \mathcal{E}_1^{*2} \bar{\rho}_{eg}), \\ \left[\frac{d}{dt} - i\Delta_1 + i\delta\omega_{eg}^F + \frac{1}{2} \left(\gamma_{eg}^F + \frac{1}{\tau_e} \right) + \frac{1}{T_{eg}} \right] \bar{\rho}_{eg} &= -i\mu_{eg} \mathcal{E}_1^2 (\rho_{gg} - \rho_{ee}). \end{aligned} \quad (3.1)$$

This adiabatic elimination assumes all time scales of our problem to be slower than $1/\Gamma_a$. The Fano profile

$$\gamma_e^F = \gamma_e^{(1)} + \gamma_e^{(2)} \left[1 + \frac{1}{2} \Gamma_a \rho_{ea}^2 \frac{(q_{ea}^2 - 1) \frac{1}{2} \Gamma_a / \beta_{ae} + 2q_{ea} \Delta_2}{\Delta_2^2 + (\frac{1}{2} \Gamma_a / \beta_{ae})^2} \right] \quad (3.2)$$

describes the resonant decay of the population of $|e\rangle$ to the continua where $\gamma_e^{(r)}$, with $r=1,2$, represent the contributions due to the first and second laser. The quadratic shift and width due to the autoionizing resonance is

$$i\delta\omega_{eg}^F + \frac{1}{2} \gamma_{eg}^F = \frac{1}{2} \gamma_e^{(1)} + \frac{1}{2} \gamma_e^{(2)} \left[1 + \frac{1}{2} \rho_{ea}^2 \Gamma_a \frac{(q_{ea} - i)^2}{-i(\Delta_1 + \Delta_2) + \frac{1}{2} \Gamma_a / \beta_{ag}} \right], \quad (3.3)$$

which again displays the characteristic interference effects. Note the different dependence on the detunings in Eqs. (3.2) and (3.3). The polarization driving the generated harmonic becomes

$$\begin{aligned} P_3(z,t) &= \sum_{i=g,e,a} \alpha_i(\omega_3) \rho_{ii}(z,t) \mathcal{E}_3(z,t) + \left[\xi_{ge} - \frac{\mu_{ga}(1-i/q_{ga})\mu_{ae}(1-i/q_{ae})}{\Delta_1 + \Delta_2 + i\frac{1}{2}\Gamma_a/\beta_{ag}} \right] \\ &\quad \times \mathcal{E}_2(z,t) \bar{\rho}_{eg}(z,t) \exp[-i\Delta k(z,t)z], \end{aligned} \quad (3.4)$$

where the second term in large parentheses is the resonant contribution from the autoionizing state. Both the density-matrix equations and polarization given above are generalizations of the results obtained by Georges *et al.*²²

IV. RATE APPROXIMATION

The purpose of this section is to provide simple analytic expressions for various limiting cases of parameter combinations for the generated harmonic and ionization probability. Although in a quantitative sense the validity of these approximations is very restricted, they often allow a quite general qualitative insight into the parameter dependences of the problem and thus complement the results of numerical calculations presented in Sec. V.

In a square-pulse approximation for $\mathcal{E}_1(t)$ and $\mathcal{E}_2(t)$ the time dependences of the density-matrix elements are determined by the eigenvalues of the Liouville matrix in Eq. (2.12). If one of its roots is smaller than the other eigenvalues, it dominates the

long-time behavior of the system; physically this means that one of the rates governing the redistribution of the electrons between the atomic levels is slower than the other ones and corresponds to a bottleneck in the excitations of the electrons. One way of isolating these slowly decaying roots is the adiabatic elimination of the fast variables in the density-matrix equations. Below we shall study in this approximation the two limiting cases of a saturated two-photon transition coupled weakly to an autoionizing resonance and a weak two-photon excitation coupled to the strongly driven system $|e\rangle, |a\rangle$.

If the second laser exciting the autoionizing resonance is weak, the adiabatic elimination of the off-diagonal density matrix elements in Eq. (3.1) leads to rate equations for the populations ρ_{ee} and ρ_{gg} , where the decay to the continuum states described by the Fano ionization rate γ_e^F [Eq. (3.2)], and the redistribution of the electrons between the ground state and the two-photon resonance is governed by the two-photon transition rate

$$W_{eg} = 2 |\mu_{eg} \mathcal{E}_1^2|^2 \text{Im} \left[\frac{-1}{\Delta_1 + i \frac{1}{2} \gamma_e^{(2)} / \beta_{eg} - \frac{|\mu_{ae} \mathcal{E}_2|^2 (1 - i/q_{ae})^2}{\Delta_1 + \Delta_2 + i \frac{1}{2} \Gamma_a / \beta_{ag}}} \right]. \quad (4.1)$$

These rate equations are valid for weak fields, if the transverse decay constants are larger than the diagonal decay rates, and describe the time-averaged behavior of the populations in the strong-field limit, where Rabi oscillations appear. If one of the rates in Eq. (3.1) dominates over the others, the time dependence of the ionization probability can be approximately described by

$$\mathcal{P}(t) = 1 - e^{-Rt} \quad (4.2)$$

with

$$R = \frac{\gamma_e^F W_{eg}}{\gamma_e^F + \frac{1}{\tau_e} + 2W_{eg}}, \quad (4.3)$$

a single time-independent ionization rate.

For a saturated two-photon transition, the ionization rate is equal to $\frac{1}{2} \gamma_e^F$, whereas for a weak bound-bound step the ionization rate equals W_{eg}

which is proportional to γ_{eg}^F [compare Eq. (3.3)]. A more rigorous derivation of the single rate approximation (4.2) for the second ionization probability is the following³¹: Starting from the Ansatz

$$\rho_{ee}(t) + \rho_{gg}(t) = e^{-Rt} \quad (4.4)$$

we determine R by requiring

$$\int_0^\infty dt [\rho_{ee}(t) + \rho_{gg}(t)] = \int_0^\infty e^{-Rt} dt = \frac{1}{R}. \quad (4.5)$$

According to its definition, R represents a global time-averaged ionization rate. By integrating the density-matrix equation (3.1) over the time, we obtain a system of linear equations for the time-integrated density-matrix elements, which is readily solved for R in agreement with Eq. (4.2). With the same approximation as in Eq. (4.2) we get

$$\bar{\rho}_{eg}(t) = \frac{-i\mu_{eg} \mathcal{E}_1^2}{-i\Delta_1 + i\delta\omega_{eg}^F + \frac{1}{2} \left(\gamma_{eg}^F + \frac{1}{\tau_e} \right) + \frac{1}{T_{eg}} \frac{\gamma_e^F}{2} + \frac{1}{\tau_e} + 2W_{eg}} \frac{\gamma_e^F}{2} + \frac{1}{\tau_e} e^{-Rt}, \quad (4.6)$$

and the energy of the harmonic becomes

$$U_3 = \frac{\omega_3^2}{2\epsilon_0 c} (NL)^2 |\xi_{ge} \mathcal{F}(\Delta_1 + \Delta_2) \mathcal{E}_2|^2 |\bar{\rho}_{eg}(t=0)|^2 F(\Delta k L, \sigma L) T_{\text{eff}}, \quad (4.7)$$

where $T_{\text{eff}} = (1 - e^{-2RT})/2R$ is the effective interaction time. In the derivation of Eq. (4.7) the time variation of $F(\Delta k L, \sigma L)$ has been neglected.

The modification of the line profile due to the (weakly excited) autoionizing resonance is contained in the Fano-type factor

$$\mathcal{F}(\Delta_1 + \Delta_2) = 1 + \frac{1}{2} \Gamma_a \frac{\rho_{ga} \rho_{ae}}{\rho_{ge}} \frac{(q_{ga} - i)(q_{ae} - i)}{(q_{ge} - i)(\Delta_1 + \Delta_2 + i \frac{1}{2} \Gamma_a / \beta_{ag})}. \quad (4.8)$$

In the low-intensity limit of the first laser and for $q_{ge} = 0$ the nonlinear susceptibility in Eq. (4.7) is in agreement with the results of Refs. 7 and 8. The saturation of the two-photon resonance, contained in the second factor of Eq. (4.6), manifests itself in a saturation dip in the resonance profile as a function of Δ_1 .^{22,25}

ac-Stark splitting of the two-photon transition occurs if the two-photon Rabi frequency exceeds the spontaneous and induced widths of $|e\rangle$. Scanning with the second laser as a probe over the autoionizing resonance, this dynamic Stark splitting can be recognized only at such extremely high intensities of the first laser, for which the two-photon Rabi frequency is larger than the width of the autoionizing structure in the continuum.

For $\Delta_1 = 0$ and $\beta_{eg} \approx \beta_{ag}$ the ionization rate is given by

$$R = \frac{1}{2} [\gamma_e^F(\Delta_2 + |\mu_{eg} \mathcal{E}_1^2|) + \gamma_e^F(\Delta_2 - |\mu_{eg} \mathcal{E}_1^2|)] \rho_{11}(\Delta_1 = 0), \quad (4.9)$$

and the energy of the generated harmonic becomes proportional to

$$\mathcal{F}(\Delta_1, \Delta_2) = \frac{|\Delta_1 + \Delta_2 + q_{ae} \frac{1}{2} \Gamma_a \beta_{eg} \rho_{ae}^2|^2 + (\frac{1}{2} \Gamma_a / \beta_{ag})^2 (1 - \beta_{eg} \beta_{ag} \rho_{ae}^2) (1 + q_{ae}^2 \beta_{ag} \beta_{eg} \rho_{ae}^2)}{[\Delta_1 + \Delta_2 - \frac{1}{2} \Gamma_a / \beta_{ag} \xi(\Delta_1)]^2 + (\frac{1}{2} \Gamma_a / \beta_{ag})^2 [1 - \eta(\Delta_1)]^2} \quad (4.12)$$

and

$$U_3 = \frac{\omega_3^2}{2\epsilon_0 c} (NL)^2 |\xi_{ge} \bar{\mathcal{F}} \mathcal{E}_2|^2 |\bar{\rho}_{eg}(0)|^2 F(\Delta k L, \sigma L) T_{\text{eff}}, \quad (4.13)$$

with

$$\bar{\mathcal{F}} = \frac{\Delta_1 + \Delta_2 + i \frac{1}{2} \Gamma_a / \beta_{ag} + \frac{1}{2} \Gamma_a \frac{\rho_{ga} \rho_{ae}}{\rho_{ge}} \frac{q_{ga} - i}{q_{ge} - i} (q_{ae} - i)}{[\Delta_1 + \Delta_2 - \frac{1}{2} \Gamma_a / \beta_{ag} \xi(\Delta_1)] + i \frac{1}{2} \Gamma_a / \beta_{ag} [1 - \eta(\Delta_1)]} \quad (4.14)$$

$$U_3 \sim |\mathcal{F}(\Delta_2 + |\mu_{eg} \mathcal{E}_1^2|)|^2 + |\mathcal{F}(\Delta_2 - |\mu_{eg} \mathcal{E}_1^2|)|^2. \quad (4.10)$$

Let us now turn to the case of a weakly excited two-photon resonance coupled to a strongly driven transition to the autoionizing resonance. Electrons excited to $|e\rangle$ are readily transferred to $|a\rangle$ and ionized into the continuum. Since the two-photon transition is the bottleneck of the excitation in the system, the populations of $|e\rangle$ and $|a\rangle$ are small. The long-time behavior is governed by the slowly decaying ground-state population $\rho_{gg}(t) \simeq e^{-RT}$, where R turns out to be identical to the bound-bound rate W_{eg} already derived in Eq. (4.1) in a different context. To study for fixed Δ_1 the dependence of the ionization rate R and the energy U_3 of the generated harmonic on the detuning Δ_2 of the second laser, both R and U_3 are conveniently written in the form^{27,32}

$$R = 2 |\mu_{eg} \mathcal{E}_1^2|^2 \frac{\frac{1}{2} \gamma_e^{(2)} / \beta_{eg}}{\Delta_1^2 + (\frac{1}{2} \gamma_e^{(2)} / \beta_{eg})^2} \mathcal{F}(\Delta_1, \Delta_2) \quad (4.11)$$

with

and the slowly varying density-matrix element in the absence of an autoionizing state,

$$\bar{\rho}_{eg}(0) = \frac{\mu_{eg} \mathcal{E}_1^2}{\Delta_1 + i \frac{1}{2} \gamma_e^{(2)} / \beta_{eg}}. \quad (4.15)$$

The modifications in the ionization and generated harmonic due to the strongly driven transition to the autoionizing state are contained in the Fano profile $\mathcal{F}(\Delta_1, \Delta_2)$ and $\overline{\mathcal{F}}$, respectively. The shift of the resonant position and width of these Fano profiles are given by

$$\xi(\Delta_1) = \frac{1}{2} \gamma_e^{(2)} \beta_{ag} \rho_{ae}^2 \frac{(q_{ae}^2 - 1) \Delta_1 - 2q_{ae} \frac{1}{2} \gamma_e^{(2)} / \beta_{eg}}{\Delta_1^2 + (\frac{1}{2} \gamma_e^{(2)} / \beta_{eg})^2} \quad (4.16)$$

and

$$1 - \eta(\Delta_1) = 1 + \frac{1}{2} \gamma_e^{(2)} \beta_{ag} \rho_{ae}^2 \frac{(\frac{1}{2} \gamma_e^{(2)} / \beta_{eg})(q_{ae}^2 - 1) + 2q_{ae} \Delta_1}{\Delta_1^2 + (\frac{1}{2} \gamma_e^{(2)} / \beta_{eg})^2}, \quad (4.17)$$

respectively.

Note that $1 - \eta(\Delta_1)$ itself is again a Fano profile as a function of Δ_1 with a minimum near $\Delta_1 = -\frac{1}{2} q_{ae} \gamma_e^{(2)} / \beta_{eg}$. Since the effective Fano parameter of the ionization modification factor $\mathcal{F}(\Delta_1, \Delta_2)$ is roughly $q_{\text{eff}} = [q_{ae} + \xi(\Delta_1)] / [1 - \eta(\Delta_1)]$, the shape of this Fano profile changes with the detuning Δ_1 . At this point the width can, at least in principle, narrow down to the collision-induced and radiative decay rates, provided that $\rho_{ae} \beta_{eg}$ is close to 1. While in the generated harmonic this narrowing appears as a strong enhancement of the resonance signal, in the ionization probability the small denominator gets (almost) cancelled by the Fano minimum in the numerator so that at this critical value $\mathcal{F}(\Delta_1, \Delta_2) \approx 1$.^{27,32}

To study for constant Δ_2 the dependence of the ionization probability and the harmonic energy on the detuning of the first (weak) laser Δ_1 , R and U_3 are conveniently written in the form¹⁹

$$R = \frac{|\mu_{eg} \mathcal{E}_1^2|^2 \frac{\gamma_e^{(2)}}{\beta_{eg}} \left| \Delta_1 + \Delta_2 + \rho_{ae}^2 / \beta_{eg} \frac{1}{2} \Gamma_a q_{ae} \right|^2 + (\frac{1}{2} \Gamma_a / \beta_{ag})^2 (1 - \beta_{eg} \beta_{ag} \rho_{ae}^2) (1 + q_{ae}^2 \beta_{ag} \beta_{eg} \rho_{ae}^2)}{|f|^2} \quad (4.18)$$

and

$$U_3 = \frac{\omega_3^2}{2\epsilon_0 c} (NL)^2 \left| \xi_{ge} \mathcal{E}_2 \mu_{eg} \mathcal{E}_1^2 \right|^2 \times \frac{\left| \Delta_1 + \Delta_2 + i \frac{1}{2} \Gamma_a / \beta_{ag} + \frac{1}{2} \Gamma_a \frac{\rho_{ga} \rho_{ae}}{\rho_{ge}} \frac{q_{ga} - i}{q_{ge} - i} (q_{ae} - i) \right|^2}{|f|^2} F(\Delta k L, \sigma L) T_{\text{eff}}. \quad (4.19)$$

The roots of the polynomial

$$f = (\Delta_1 + i \frac{1}{2} \gamma_e^{(2)} / \beta_{eg}) (\Delta_1 + \Delta_2 + i \frac{1}{2} \Gamma_a / \beta_{ag}) - |\mu_{ae} \mathcal{E}_2|^2 (1 - i / q_{ae})^2 \quad (4.20)$$

determine the positions and widths of the resonance lines. Generally, both R and U_3 will therefore exhibit a two-peaked structure. If the strong second laser is tuned off resonance, one resonance line appears near $\Delta_1 + \Delta_2 = 0$ corresponding to the nonresonant three-photon excitation of the autoionizing state, while the second peak near $\Delta_1 = 0$ is a contribution due to a stepwise excitation via the two-photon resonance.

For near-resonance conditions of the second laser both the ionization probability and the harmonic energy exhibit ac-stark splitting in the intensity regime where the Rabi frequency $\Omega_{ae} = 2\mu_{ae} \mathcal{E}_2$ exceeds both, the autoionization width and the induced ionization widths of $|e\rangle$ and $|a\rangle$, according to

$$R = \frac{|\mu_{eg} \mathcal{E}_1^2|^2}{(1 + q_{ae}^2) \Gamma_a} \left| -\frac{\Delta_1^+ + \frac{1}{2} \Gamma_a q_{ae}}{\Delta_1 - \Delta_1^+} + \frac{\Delta_1^- + \frac{1}{2} \Gamma_a q_{ae}}{\Delta_1 - \Delta_1^-} \right|^2 \quad (4.21)$$

and

$$U_3 = \frac{\omega_3^2}{2\epsilon_0 c} (NL)^2 \frac{|\xi_{ge} \mathcal{E}_2 \mu_{eg} \mathcal{E}_1^2|^2}{4 |\mu_{ae} \mathcal{E}_2|^2 \left[1 + \frac{1}{q_{ae}^2} \right]} \left| - \frac{\Delta_1^+ + \frac{1}{2} \Gamma_a \left[i + \frac{\rho_{ga} q_{ga} - i}{\rho_{ge} q_{ge} - i} (q_{ae} - i) \right]}{\Delta_1 - \Delta_1^+} + \frac{\Delta_1^- + \frac{1}{2} \Gamma_a \left[i + \frac{\rho_{ga} q_{ga} - i}{\rho_{ge} q_{ge} - i} (q_{ae} - i) \right]}{\Delta_1 - \Delta_1^-} \right|^2 F(\Delta k L, \sigma L) T_{\text{eff}}, \quad (4.22)$$

with

$$\Delta_1^+ = |\mu_{ae} \mathcal{E}_2| - i \left[\frac{1}{4} (\Gamma_a + \gamma_e^{(2)}) + \frac{|\mu_{ae} \mathcal{E}_2|}{q_{ae}} \right],$$

$$\Delta_1^- = -|\mu_{ae} \mathcal{E}_2| - i \left[\frac{1}{4} (\Gamma_a + \gamma_e^{(2)}) - \frac{|\mu_{ae} \mathcal{E}_2|}{q_{ae}} \right].$$

In these formulas we have assumed ρ_{ae} , β_{ag} , and β_{eg} to be close to 1. Note that as a result of interference the widths of both Stark-split dressed states are different. With increasing intensity of the second laser the width of the second line has a minimum when $\gamma_e^{(2)} \approx \Gamma_a$. At this critical intensity the corresponding dressed state becomes quasistable against a decay to the continua.^{19,33} The small width, however, leads to a strongly peaked resonance line in the energy of the generated harmonic. The experimental realization of the line shape (4.11) and (4.13) heavily depends on the condition according to which both the autoionization and ionization decay are saturated in time ($\Gamma_a T \gg 1$, $\gamma_e T \gg 1$). For interaction times and intensities such that $\gamma_e T \ll 1$ but $\Gamma_a T \gg 1$, a short time expansion of the density-matrix equations (2.12) ($|\mu_{eg} \mathcal{E}_1^2|$, $|\Delta_1| \ll 1/T$) shows that both, the ionization probability

$$P(T) = \gamma_e^{F \frac{1}{3}} |\mu_{ef} \mathcal{E}_1^2|^2 T^3 \quad (4.23)$$

and the energy of the generated harmonic

$$U_3 = \frac{\omega_3^2}{2\epsilon_0 c} (NL)^2 |\xi_{ge} \mathcal{E}_2 \mathcal{S}(\Delta_1 + \Delta_2)|^2 \frac{1}{3} |\mu_{eg} \mathcal{E}_1^2|^2 T^3 F(\Delta k L, \sigma L), \quad (4.24)$$

are characterized by the Fano profiles, which we already found in the limit of perturbation theory of a weak second laser [see Eqs. (3.2) and (4.8)].

V. NUMERICAL RESULTS

To illustrate typical line profiles in multiphoton ionization and harmonic generation we present in this section results obtained by numerical integration of the density-matrix equations (2.12), assuming a square-pulse shape of length T for both \mathcal{E}_1 and \mathcal{E}_2 . To separate the atomic contribution to the generated harmonic line shape, represented by $\bar{\rho}_{eg}$

and $\bar{\rho}_{ag}$ in Eq. (2.12), from contributions due to pulse propagation effects, we have assumed throughout this section that $F(\Delta k L, \sigma L) = 1$. Physically, this corresponds to the restriction to low atomic densities or very short cells, i.e., $|\Delta k(0, t)| L \ll 1$ and $\sigma(0, t) L \ll 1$; this neglects the change of the phase mismatch with the redistribution of the atomic populations. In view of the results of Ref. 22 we expect the time-dependent

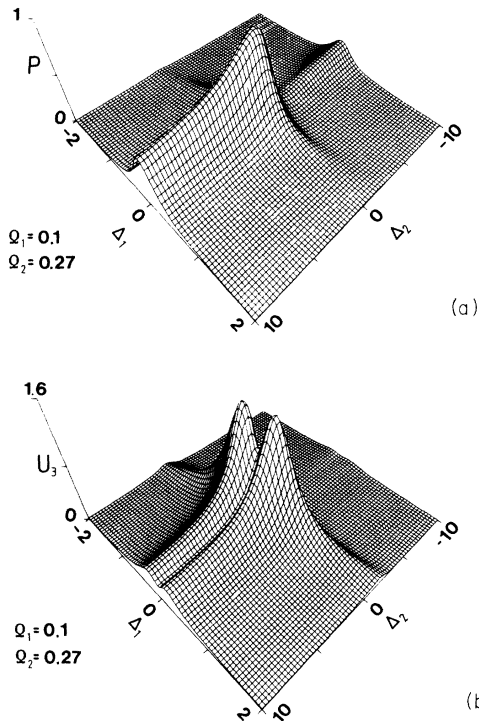


FIG. 2. Ionization probability and the harmonic energy is plotted as a function of (a) Δ_1 and (b) Δ_2 , respectively. The first transition is saturated ($\Omega_1 = 2 |\mu_{eg} \mathcal{E}_1^2| = 0.1 \Gamma_a$), while the coupling to the autoionizing state is weak ($\Omega_2 = 2 |\mu_{ae} \mathcal{E}_2| = 0.27 \Gamma_a$).

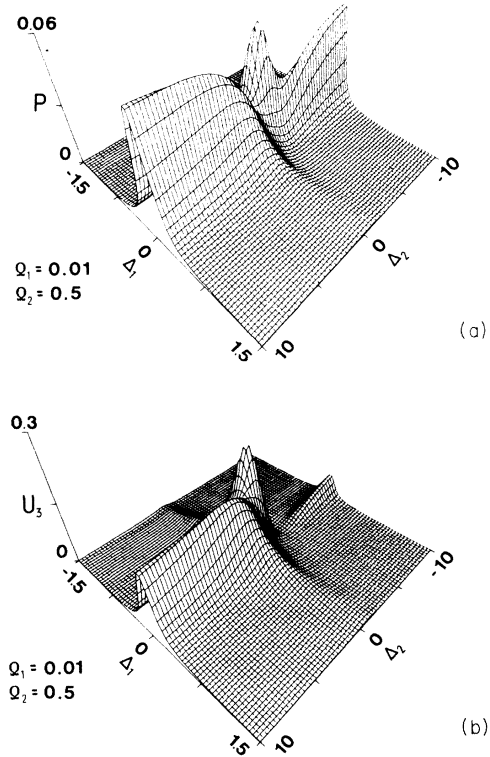


FIG. 3. (a) Ionization probability and (b) harmonic energy. The first transition is weak ($\Omega_2 = 0.01 \Gamma_a$), while the second transition is almost saturated ($\Omega_2 = 0.5 \Gamma_a$).

phase-matching function only to introduce some additional asymmetries in the resonance profiles.

We assume below a model atom with an autoionization width of $\Gamma_a = 10^{12} \text{ s}^{-1}$. All other atomic parameters are chosen as follows:

$$\frac{1}{2} \frac{1}{\tau_a} = \frac{1}{\tau_e} = \frac{1}{\tau_{ag}} = \frac{1}{\tau_{ae}} = 2 \times 10^{-3} \Gamma_a,$$

$$\frac{1}{T_{eg}} = \frac{1}{T_{ag}} = \frac{1}{T_{ae}} = 2 \times 10^{-2} \Gamma_a,$$

$$\gamma_a = 0.1 |2\mu_{eg} \mathcal{E}_1|^2 + \gamma_e^{(2)},$$

$$\gamma_e^{(1)} = 0,$$

$$T = 100/\Gamma_a.$$

The Fano parameters are taken to be $q_{ae} = q_{ga} = 3$ and $q_{ge} = 2$ with the corresponding correlation coefficients $\rho_{ae} = \rho_{ga} = \rho_{ge} = 0.9$.

Figures 2(a) and 2(b) show the dependence of the ionization probability $P(T)$ and the generated harmonic energy in units of

$$(\omega_3^2/2\epsilon_0 c)(NL)^2 (|\xi_{ge}|^2/|\mu_{ae}|^2)^{1/2} \Gamma_a$$

on the detunings of the first and second laser Δ_1 and Δ_2 (in units of $\Gamma_a/2$). The first laser saturates the two-photon resonance, but the laser-induced coupling to the autoionizing state is still weak. As expected from Eqs. (4.3) and (4.7) the resonance lines have the form of asymmetric Fano profiles as a function of Δ_2 , which are characteristic of weakly excited autoionizing states.^{1,17-20} The resonance profile of the ionization signal is a power-broadened symmetric Lorentzian as a function of the detuning Δ_1 . In Fig. 2(b) we recognize a saturation dip in the energy of the generated harmonic. Near resonance $\Delta_2 \approx 0$, the two peaks are somewhat asymmetric as a function of Δ_1 caused by interference effects in the autoionizing transition. In contrast we note that the asymmetry found by Georges *et al.*²² is a consequence of the time dependence of the phase mismatch [see Eqs. (2.23) and (2.24)].

Beside the dominant resonance in Figs. 2(a) and 2(b), at $\Delta_1 \approx 0$ which corresponds to the stepwise excitation

$$|g\rangle \xrightarrow{\omega_1} |e\rangle \xrightarrow{\omega_2} |a\rangle,$$

there is a second much weaker and broader structure at $\Delta_1 + \Delta_2 \approx 0$ which is associated with the direct three-photon transition to the autoionizing state.

The ionization probability and harmonic production for a weakly excited two-photon resonance coupled to an almost saturated autoionizing state is plotted in Figs. 3(a) and 3(b), respectively. In agreement with Eq. (4.11) for constant Δ_1 the resonance line shapes of the ionization signal as a function of Δ_2 are Fano profiles with the widths, the effective Fano q parameters, and the positions of the maxima critically depending on the intensity and the detuning Δ_1 . Similarly, the resonance behavior of the harmonic energy can be understood on the basis of Eq. (4.13). The appearance of peaks in Figs. 3(a) and 3(b) is related to the Fano minimum of the width function $1 - \eta(\Delta_1)$ in Eqs. (4.12) and (4.14). Note that such a peak will exist in the ionization probability only for $\rho_{ae}\beta_{ag}\beta_{eg} \neq 1$.³² While off resonance ($\Delta_2 \neq 0$), the line shape Δ_1 is practically symmetric; there is some asymmetric broadening at $\Delta_2 = 0$.

Harmonic generation for a saturated two-photon resonance followed by a strongly driven transition to an autoionization state (Fig. 4) has features from both Figs. 2(b) and 3(b). We do not show the corresponding ionization probability since, with the exception of the increase of the resonance width in Δ_1 and the total amount of ionized atoms, the resonance structure is similar to that of Fig. 3(a). Near the resonance of both lasers, the doublet structure of Fig. 2(b) and the peak discussed in the context of Fig. 3(b) coalesce into a single broad asymmetric resonance profile.

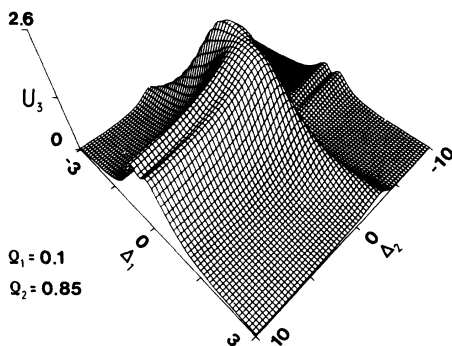


FIG. 4. Harmonic energy for $\Omega_1 = 0.1\Gamma_a$ and $\Omega_2 = 0.85\Gamma_a$. The corresponding ionization probability is not plotted since it is qualitatively similar to Fig. 3(a).

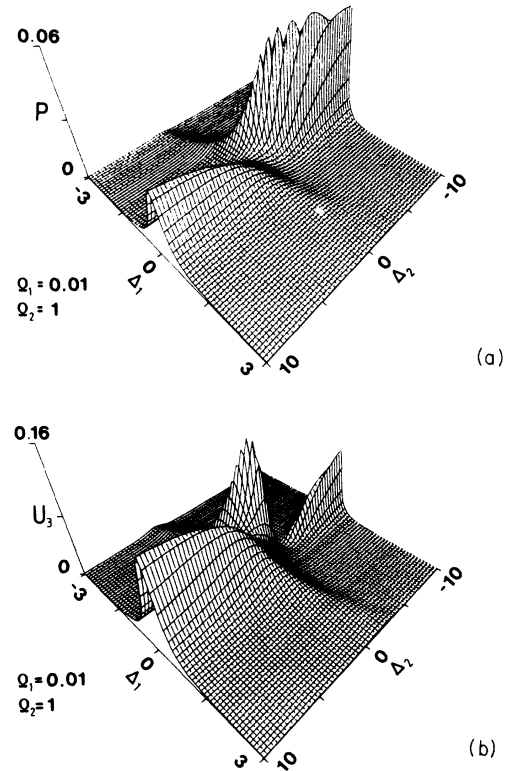


FIG. 5. (a) Ionization probability and (b) harmonic energy. The first transition is weak ($\Omega_1 = 0.01\Gamma_a$), while the second transition is saturated ($\Omega_2 = \Gamma_a$).

In Figs. 5(a) and 5(b) we have plotted the ionization probability and harmonic energy for a weakly excited two-photon resonance coupled to a strongly saturated transition to the autoionizing state. In comparison to Figs. 3(a) and 3(b), the intensity of the second laser is increased by a factor of 4. On resonance, $\Delta_2 = 0$, the ionization probability now exhibits ac-Stark splitting as a function of Δ_1 . As a result of interference effects both Stark-split states have different width [compare Eq. (4.21)]. The peak in Fig. 3(a) has now given place to a narrow resonance structure with its height quickly decreasing towards $\Delta_2 = 0$. Asymmetric ac-Stark splitting is also observable in the harmonic signal. Note that with increasing saturation the conversion efficiency becomes smaller.

Finally, Fig. 6 shows the harmonic signal for saturation of the first and second transition. The ac-Stark-split lines are now extremely broad, but the interference minima are still well visible.

VI. CONCLUSIONS

In this paper we have studied intensity effects in harmonic generation and multiphoton ionization

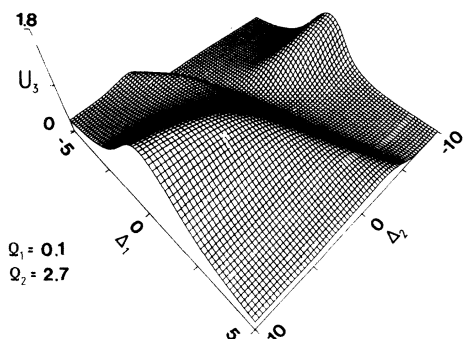


FIG. 6. Harmonic energy for $\Omega_1=0.1\Gamma_a$ and $\Omega_2=2.7\Gamma_a$. Both transitions are saturated.

via a two-photon resonance coupled to an autoionizing state. In harmonic generation autoionizing resonances may lead to a considerable enhancement of the harmonic production, compared to the off-resonance value. In general, the saturation of the resonances decreases the conversion efficiency; the optimum intensities for the injected laser powers will be to work at the onset of saturation. Note, however, that the resonant enhancements predicted in this paper depend on the assumption of a low-density gas (or, equivalently, short cells). From the point of view of conversion efficiencies, non-resonant phase-matched wave mixing in long cells with high densities may still be more effective.²⁵

Observation of the line shape of the generated harmonic energy provides considerable information

regarding the behavior of autoionizing states in strong laser fields, complementing the results obtained for multiphoton ionization. At low intensities of the second laser which couples the two-photon resonance to the autoionizing state, the resonance curves are intensity-independent Fano-type profiles as a function of Δ_2 .

Saturation of the two-photon resonance leads to power broadening of the ionization probability and yields a saturation dip in the generated harmonic as a function of the detuning Δ_1 of the first laser. A weak excitation of the two-photon resonance followed by a strong coupling to the autoionizing state results in Fano-type profiles in Δ_2 with line shapes and width critically depending on the intensities and the detuning Δ_1 .^{27,32} As a function of Δ_1 , ac-Stark splitting of the autoionizing transition into dressed states with different widths is observed.¹⁹ The saturation of both the first and second transition leads to a considerable broadening and washing out of the resonance structures.

ACKNOWLEDGMENTS

We thank Professor P. Lambropoulos for helpful discussions and Professor F. Ehlotzky for his continuous interest and support. This work was supported by a grant from the Jubiläumsfonds of the Österreichische Nationalbank under Contract No. 1923.

APPENDIX

In this appendix we give an outline of the derivation of the effective Hamiltonian (2.2) describing the time evolution of an atom within the gas and of the mean polarization entering Eq. (2.16). Thereby we shall make the following assumptions:

(1) $\mathcal{E}_j(z,t)$ is time independent. The generalization of our derivation to slowly varying time-dependent amplitudes $\mathcal{E}_j(z,t)$ is straightforward and does not change our results.

(2) The wave vectors $k_j(z,t)$ are slowly varying functions of time ($\omega_j/c \gg |\partial k_j(z,t)/\partial t|$).

(3) The generated harmonic is neglected in the time evolution of the atom in comparison with the incident waves. Its action on the field-induced mean polarization $P_3(z,t)$ is taken into account perturbatively.

We have to solve the Schrödinger equation with the semiclassical Hamiltonian $H=H_0+V+D$ and the initial condition $|\psi\rangle_{t=0}=|g\rangle$ neglecting the generated harmonic \mathcal{E}_3 . According to Floquet's theorem³⁴ the transition amplitudes may be written as

$$\langle j|\psi\rangle_t = -\frac{1}{2\pi i} \int_{-\infty}^{\infty} dx e^{-ixt} \sum_{n,m=-\infty}^{\infty} \langle j,-n,-m|G(x+i\epsilon)|g,0,0\rangle \\ \times \exp\{-in[\omega_1 t - k_1(z,t)z]\} \exp\{-im[\omega_2 t - k_2(z,t)z]\} \quad (\text{A1})$$

with the resolvent operator

$$G(x+i\epsilon) = \frac{1}{x+i\epsilon-H^F}.$$

The quantities $|j, -n, -m\rangle$ are Floquet states,³⁴ H^F is the corresponding Floquet Hamiltonian³⁴ and $|j\rangle$ is an arbitrary atomic state.

According to Fig. 1 the coupling between the energetically degenerate states $|g, 0, 0\rangle$, $|e, -2, 0\rangle$, $|a, -2, -1\rangle$, and $|E_\alpha, -2, -1\rangle$ must be treated exactly. The influence of all other Floquet states can be taken into account perturbatively. With the help of the projection operator

$$P = |g, 0, 0\rangle\langle g, 0, 0| + |e, -2, 0\rangle\langle e, -2, 0| + |a, -2, -1\rangle\langle a, -2, -1| + \sum_\alpha \int dE_\alpha |E_\alpha, -2, -1\rangle\langle E_\alpha, -2, -1|, \quad (\text{A2})$$

we restrict the resolvent on the subspace of the resonant states

$$PG(x + i\epsilon)P = \frac{1}{x + i\epsilon - H_{\text{eff}}^F}, \quad (\text{A3})$$

where H_{eff}^F is given in pole approximation¹⁹ by

$$H_{\text{eff}}^F = PH^FP + PH^FQ \frac{1}{\omega_g + i\epsilon - QH^FQ} QH^FP \quad (\text{A4})$$

and $Q = 1 - P$. We chose our relevant atomic states so that

$$\begin{aligned} (H_0 + V)|g\rangle &= \omega_g |g\rangle, \\ (H_0 + V)|e\rangle &= \omega_e |g\rangle, \\ (H_0 + \langle a|V|a\rangle)|a\rangle &= \omega_a |a\rangle, \\ Q_a(H_0 + V)Q_a|E_\alpha\rangle &= E_\alpha |E_\alpha\rangle \end{aligned} \quad (\text{A5})$$

with

$$Q_a = 1 - |a\rangle\langle a|.$$

Substituting Eq. (A3) into (A1) we keep the coupling to the electromagnetic field in Q space up to second-order perturbation theory. Eliminating $\langle E_\alpha, -2, -1|G(x + i\epsilon)|g, 0, 0\rangle$ in the pole approximation and neglecting field-induced continuum-continuum transitions we find a Schrödinger equation in the atomic subspace $|g\rangle$, $|e\rangle$, and $|a\rangle$ with the effective Hamiltonian given by Eq. (2.2).

The complex polarizability of the autoionizing resonance $|a\rangle$ due to the first laser is given by

$$\alpha_a(\omega_1) = - \left\langle \psi_a^+ \left| \left[\vec{\mu} \cdot \vec{e}_1 \frac{1}{\omega_a - \omega_1 - H_A + i\epsilon} \vec{\mu} \cdot \vec{e}_1^* + \vec{\mu} \cdot \vec{e}_1^* \frac{1}{\omega_a + \omega_1 - H_A + i\epsilon} \vec{\mu} \cdot \vec{e}_1 \right] \right| \psi_a^+ \right\rangle \quad (\text{A6})$$

with

$$|\psi_a^\pm\rangle = |a\rangle + Q_a \frac{1}{\omega_a - H_A \pm i\epsilon} Q_a V |a\rangle.$$

For the modified atomic polarizability caused by the second laser we find

$$\bar{\alpha}_a(\omega_2) = - \left\langle \psi_a^+ \left| \left[\vec{\mu} \cdot \vec{e}_2 Q_e \frac{1}{\omega_a - \omega_2 - H_A + i\epsilon} Q_e \vec{\mu} \cdot \vec{e}_2^* + \vec{\mu} \cdot \vec{e}_2^* \frac{1}{\omega_a + \omega_2 - H_A + i\epsilon} \vec{\mu} \cdot \vec{e}_2 \right] \right| \psi_a^+ \right\rangle \quad (\text{A7})$$

with $Q_e = 1 - |e\rangle\langle e|$.

The shift of the autoionizing resonance due to the configuration interaction is

$$\delta\omega = \langle a | V \frac{P}{\omega_a - H_A} V | a \rangle. \quad (\text{A8})$$

The expressions for all other parameters determining the time evolution of the atom may be found in Sec. II A. The mean atomic polarization is defined by

$$\langle \vec{P} \rangle_{z,t} = \langle \psi | \vec{\mu} | \psi \rangle_t,$$

with

$$|\psi\rangle_t = \sum_{n,m,s=-\infty}^{\infty} \langle 1, -n, -m, -s | e^{-i\tilde{H}F_t} | g, 0, 0 \rangle \exp\{-in[\omega_1 t - k_1(z,t)z]\} \\ \times \exp\{-im[\omega_2 t - k_2(z,t)z]\} \exp\{-is[(2\omega_1 + \omega_2)t - k_3(z,t)z]\}. \quad (\text{A9})$$

The Floquet Hamiltonian \tilde{H}^F now includes the generated harmonic. In lowest-order perturbation theory of the electric field and in pole approximation we find after a trivial but lengthy calculation the expressions (2.17), (2.26), and (2.27) for the polarizations $P_k(z,t)$ of our gaseous medium.

-
- ¹U. Fano, Phys. Rev. 124, 1866 (1961).
²U. Fano and J. W. Cooper, Rev. Mod. Phys. 40, 441 (1968).
³W. Mehlhorn, Electron Spectroscopy of Auger and Autoionizing States: Experiment and Theory Lecture Notes, University of Aarhus (1978) (unpublished).
⁴W. E. Cooke, T. F. Gallagher, S. A. Edelstein, and R. M. Hill, Phys. Rev. Lett. 40, 178 (1978); W. E. Cooke and T. F. Gallagher, *ibid.* 41, 1648 (1978); T. F. Gallagher, K. A. Safinya, and W. W. Cooke, Phys. Rev. A 24, 601 (1981).
⁵P. Esherick, Phys. Rev. A 15, 1920 (1977).
⁶R. T. Hodgson, P. P. Sorokin, and J. J. Wynne, Phys. Rev. Lett. 32, 343 (1974).
⁷J. A. Armstrong and J. J. Wynne, Phys. Rev. Lett. 33, 1183 (1974); P. P. Sorokin, J. J. Wynne, J. A. Armstrong, and R. T. Hodgson, Ann. N.Y. Acad. Sci. 267, 30 (1976).
⁸L. Armstrong, Jr., and B. L. Beers, Phys. Rev. Lett. 34, 1290 (1975).
⁹S. C. Wallace and G. Zdasiuk, Appl. Phys. Lett. 28, 449 (1976).
¹⁰G. S. Bjorklund, J. E. Bjorkholm, R. R. Freeman, and P. F. Liao, Appl. Phys. Lett. 31, 330 (1977).
¹¹S. L. Chin, D. Feldmann, J. Krautwald, and K. H. Welge, J. Phys. B 14, 2353 (1981).
¹²A. S. Naquvi, M. Y. Mirza, D. J. Semple, and W. W. Duley, Opt. Commun. 37, 356 (1981).
¹³G. I. Bekov, E. P. Vidolova-Angelova, L. N. Ivanov, V. S. Letokhov, and V. I. Mishin, Opt. Commun. 35, 194 (1980); Zh. Eksp. Teor. Fiz. 80, 866 (1981) [Sov. Phys.—JETP 53, 441 (1981)].
¹⁴For a few representative papers see Refs. 4, 5, 11, 12, and 13.
¹⁵We are not concerned with field-induced autoionizing-like resonances in this paper as discussed by L. Armstrong, Jr., B. L. Beers, and S. Feneuille, Phys. Rev. A 12, 1903 (1975); Yu. I. Heller and A. K. Popov, Opt. Commun. 18, 449 (1976); Yu. I. Heller, V. F. Lukinykh, A. K. Popov, and V. V. Slabko, Phys. Lett. 82A, 4 (1981); and see Ref. 33.
¹⁶P. Lambropoulos, Adv. Atom. Mol. Phys. 12, 87 (1976); S. Swain, Adv. Atom. Mol. Phys. 16, 159 (1980).
¹⁷P. Lambropoulos, Appl. Opt. 19, 3926 (1980).
¹⁸V. S. Lisitsa and S. I. Yakovlenko, Zh. Eksp. Teor. Fiz. 66, 1981 (1974) [Sov. Phys.—JETP 39, 975 (1974)].
¹⁹P. Lambropoulos and P. Zoller, Phys. Rev. A 24, 379 (1981).
²⁰K. Rzazewski and J. H. Eberly, Phys. Rev. Lett. 47, 408 (1981).
²¹C. R. Vidal, Appl. Opt. 19, 3897 (1980).
²²A. T. Georges, P. Lambropoulos, and J. H. Marburger, Phys. Rev. A 15, 300 (1977).
²³J. N. Elgin and G. H. New, J. Phys. B 11, 3439 (1978).
²⁴J. C. Diels and A. T. Georges, Phys. Rev. A 19, 1589 (1979).
²⁵H. Puell, H. Scheingraber, and C. R. Vidal, Phys. Rev. A 22, 1165 (1980).
²⁶D. S. Betume, Phys. Rev. A 23, 3139 (1981); 25, 2845 (1982).
²⁷Yu. I. Heller and A. K. Popov, Phys. Lett. 56A, 453 (1976).
²⁸For experiments concerning the competition between the process of third-harmonic generation and multiphoton ionization in the case of an intermediate three-photon resonance, see J. C. Miller, R. N. Compton, M. G. Payne, and W. W. Garrett, Phys. Rev. Lett. 45, 114 (1980); J. C. Miller and R. N. Compton, Phys. Rev. A 25, 2056 (1982).
²⁹L. Armstrong, Jr., C. E. Theodosiou, and M. J. Wall, Phys. Rev. A 18, 2538 (1978).
³⁰I. S. Aleksakhin, G. G. Bogachev, I. P. Zapesochnyi, and S. Yu. Ugrin, Zh. Eksp. Teor. Fiz. 80, 2187 (1981) [Sov. Phys.—JETP 53, 1140 (1981)].
³¹J. J. Yeh and J. H. Eberly, Phys. Rev. A 24, 888 (1981).
³²Yu. I. Heller and A. K. Popov, Opt. Commun. 38, 345 (1981).
³³P. E. Coleman and P. L. Knight, J. Phys. B 15, L235 (1982).
³⁴J. H. Shirley, Phys. Rev. B 138, 979 (1965).

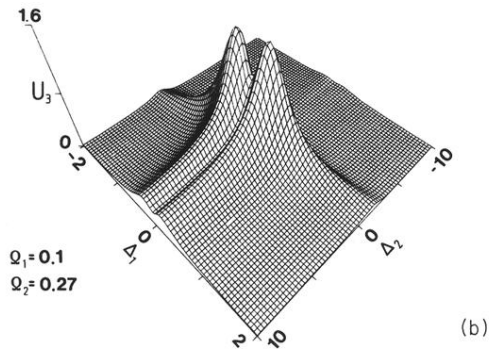
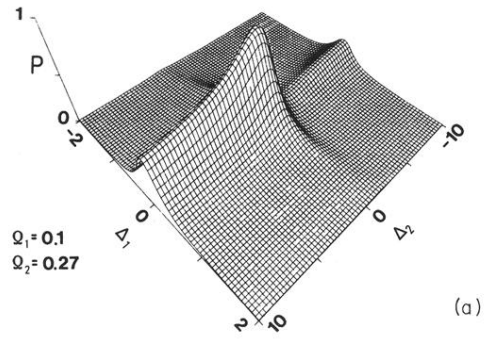


FIG. 2. Ionization probability and the harmonic energy is plotted as a function of (a) Δ_1 and (b) Δ_2 , respectively. The first transition is saturated ($\Omega_1 = 2 |\mu_{eg} \mathcal{E}_1^2| = 0.1 \Gamma_a$), while the coupling to the autoionizing state is weak ($\Omega_2 = 2 |\mu_{ae} \mathcal{E}_2| = 0.27 \Gamma_a$).

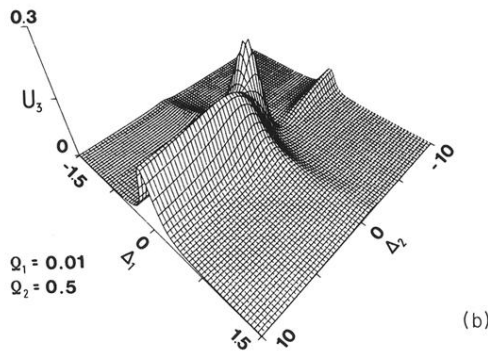
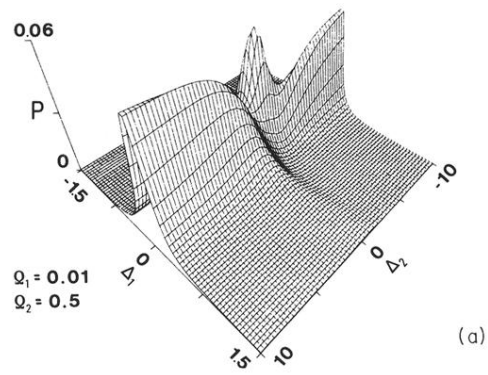


FIG. 3. (a) Ionization probability and (b) harmonic energy. The first transition is weak ($\Omega_2=0.01\Gamma_a$), while the second transition is almost saturated ($\Omega_2=0.5\Gamma_a$).

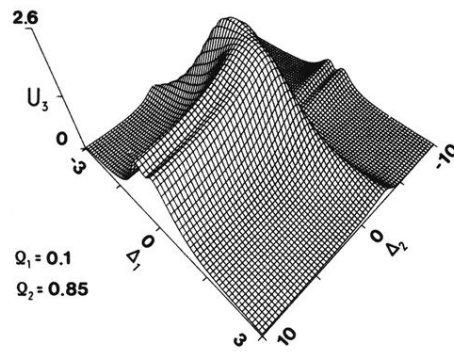


FIG. 4. Harmonic energy for $\Omega_1=0.1\Gamma_a$ and $\Omega_2=0.85\Gamma_a$. The corresponding ionization probability is not plotted since it is qualitatively similar to Fig. 3(a).

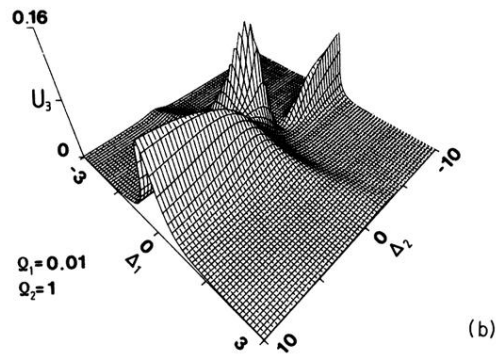
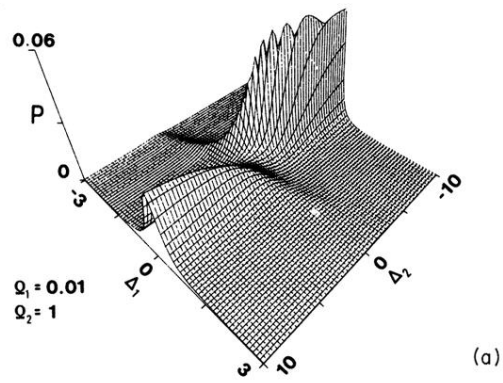


FIG. 5. (a) Ionization probability and (b) harmonic energy. The first transition is weak ($\Omega_1=0.01\Gamma_a$), while the second transition is saturated ($\Omega_2=\Gamma_a$).

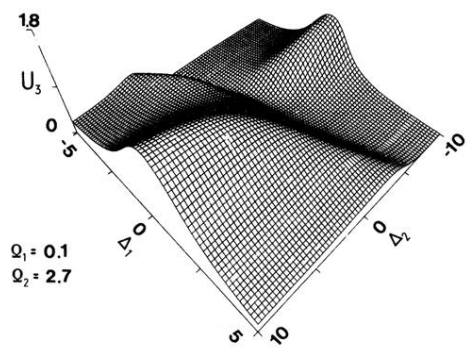


FIG. 6. Harmonic energy for $\Omega_1=0.1\Gamma_a$ and $\Omega_2=2.7\Gamma_a$. Both transitions are saturated.